DEVELOP Technical Report

Garissa County Ecological Conservation

Mapping and Characterizing Invasive Shrub Encroachment across Kenyan Savannas to Protect Endangered Hirola Antelope Habitat

Spring 2025 | Colorado – Fort Collins April 4th, 2025

Authors: Nancy Nthiga – Project Lead (Analytical Mechanics Associates), Jessica Sirois (Analytical Mechanics Associates), Angie Cruz (Analytical Mechanics Associates), Raj Yadav (Analytical Mechanics Associates)

Abstract:

The hirola (Beatragus hunteri) is a critically endangered antelope in Kenya with fewer than 250 remaining. The rinderpest disease that originally decimated their population was eradicated, but research has shown that woody encroachment has hampered species recovery by reducing the rangeland habitat this species requires. However, research quantifying rates of encroachment are limited. An understanding of these woody encroachment trends is important for the Hirola Conservation Program (HCP), a nonprofit working to conserve the hirola. We used Earth observation data (Landsat 5 Thematic Mapper, Landsat 8 Operational Land Imager, Landsat 9 Operational Land Imager-2, NASA Shuttle Radar Topography Mission; 30 m pixels and Esri Wayback Imagery; 15 m pixels) to quantify encroachment over time. We used Landsat datasets to calculate Normalized Difference Vegetation Index and Tasseled Cap Transformation, which served as predictor variables in our random forest model, along with woody cover data from the HCP and woody cover training data. Our model estimated a 37% increase in woody vegetation within the hirola's range from 1987–2025 and a 62% increase from 2017–2025. We calculated a Root Mean Square Error of 6.5% and an adjusted R² value of 0.913, indicating high prediction accuracy of the model. Due to a lack of training data for 1987, the prediction for 2017–2025 is more reliable. Our work showed that it is feasible to use remote sensing to map woody encroachment, but it has some limitations, mainly in mapping the spread of specific species. The results from this study will allow the HCP to assess encroachment trends over time within the hirola's range to inform targeted restoration efforts.

Key Terms: Hirola, Tasseled Cap Transformation, Normalized Difference Vegetation Index, woody vegetation change, habitat, random forest, remote sensing, Landsat,

Advisors: Nicholas Young (Colorado State University, Natural Resource Ecology Laboratory) Anthony Vorster (Colorado State University, Natural Resource Ecology Laboratory)

Lead: Katie Miller (California – Ames)

1. Introduction

1.1 Background Information

The hirola antelope (Beatragus hunter) is the most endangered species of antelope in the world. Native to the semi-arid savannahs of East Africa, hirola are vital in maintaining the ecosystem balance on the border of Kenya and Somalia. Historically, the geographic range of the hirola spanned eastern Kenya and southwestern Somalia across approximately 38,400 km² (Ali et al., 2017). However, the hirola has seen a rapid population decline, with fewer than 250 remaining as of 2020 (Jowers, 2020). This decline can be attributed to a combination of rangeland degradation and disease, which rendered the population endangered. (Ali et al., 2017; Ali et al., 2018). The hirola antelope's current state of endangerment has been exacerbated by a combination of top-down forces, such as predation, and bottom-up pressures, including habitat loss caused by woody tree encroachment on native grasslands. Additional factors, such as climate change and overgrazing, add to the combination of stressors on the hirola population (Ali et al., 2018). This is especially evident on the northeastern border of Kenya where approximately 43-53% of suitable grassland habitat has been encroached upon by woody vegetation. (Ali et al., 2017). Prosopis juliflora is the dominant invasive species in northern Kenya. Native to South America, Prosopis juliflora was first introduced to East Africa in the early 1980s to combat desertification (Kosgei et al., 2022). It is an extremely drought-tolerant and widespread tree species, occurring in relatively small or narrow patches and often mixed with natural vegetation or agriculture (Ng et al., 2016). Due to the complex factors contributing to the hirola's habitat loss, identifying the extent and spread of woody vegetation encroachment, as well as analyzing historical patterns of invasive species, such as Prosopis juliflora, is paramount to guiding conservation and management efforts for the hirola.

1.2 Scientific Basis

In recent years, remote sensing technologies have made it increasingly feasible to detect woody vegetation encroachment in grassland habitats by integrating Earth observation data with field observations. These advancements have significantly improved labor-intensive field survey techniques typically used to monitor these changes. These advancements have enabled the mapping of fractional woody cover within savannahs using Earth observation data (Higginbottom, 2018). Moreover, Landsat datasets have become increasingly essential for Earth observation and monitoring applications, especially within the last decade (Young et al., 2017). Given the complexities of detecting and mapping woody vegetation, leveraging advanced classification techniques is crucial for enhancing accuracy and reliability in vegetation analysis.

The fragmented distribution of woody vegetation poses challenges for detection and mapping, necessitating advanced classification techniques. Machine learning algorithms, such as the Random Forest (RF) classifier, can improve accuracy and validation of results (Breiman, 2001) Additionally, the Tasseled Cap Transformation (TCT) is a resourceful tool for monitoring various vegetation types. By compressing spectral data into a few bands associated with physical scene characteristics of the data, TCT minimizes information loss (Baig et al., 2014). It transforms original data into three indices; brightness, greenness, and wetness, which can reflect the state of vegetation and soil (Sheng et al., 2011). By integrating machine learning algorithms with spectral transformation techniques, researchers can improve the precision of woody vegetation mapping, ultimately enhancing landscape monitoring and conservation efforts.

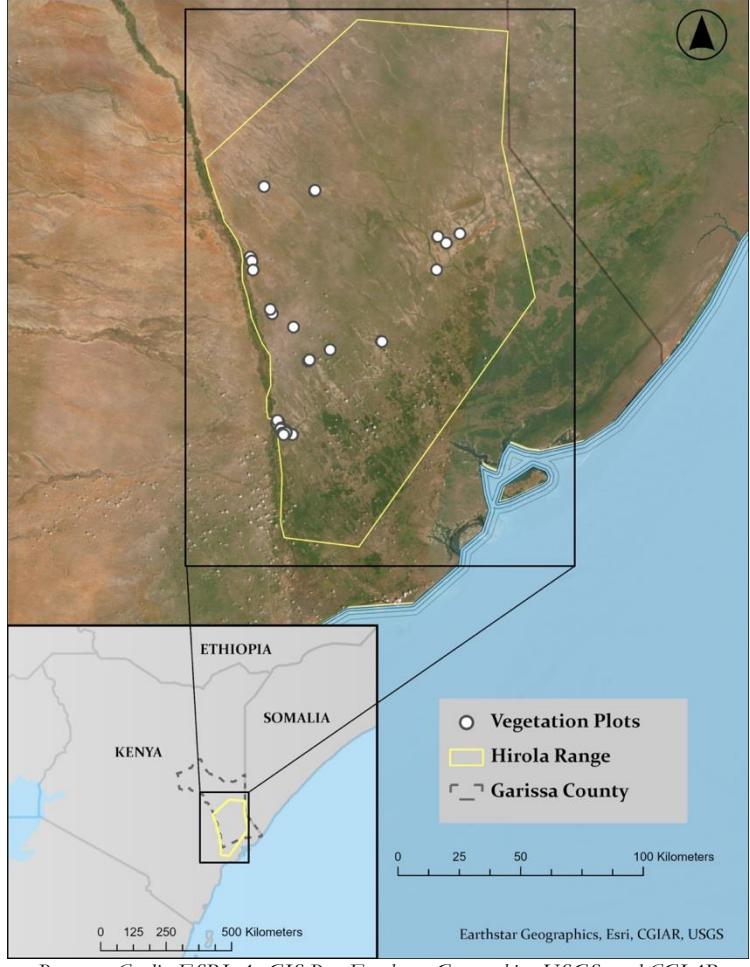
1.3 Project Partners & Objectives

Our project partnered with the Hirola Conservation Program (HCP), a non-profit organization founded by Dr. Abdullahi Ali and dedicated to the conservation of the hirola antelope and its habitat. HCP employs an adaptive management approach, integrating scientific research with local indigenous knowledge to restore and protect critical grassland ecosystems. HCP has implemented several conservation strategies, including field-based habitat monitoring, community engagement, experimental restoration projects (e.g., shrub removal, reseeding), and policy advocacy (HCP, 2023–2024 Annual Report). However, the lack of comprehensive, large-scale spatial data on shrub encroachment has limited their ability to implement targeted interventions at

the landscape level. This project has addressed this critical need by providing HCP with high-resolution spatial and ecological insights derived from Earth observation data and advanced modeling techniques. Specifically, this project aimed to map and quantify woody vegetation change to identify invasion hotspots and guide habitat restoration efforts; develop high-resolution maps of *Prosopis juliflora* extent to inform targeted removal and conservation interventions; and analyze spatiotemporal trends in woody vegetation expansion to characterize landscape changes and assess ecological impacts. Assessing the feasibility of these objectives using remote sensing informed the essential goal of our project, and these data-driven products empower HCP to make informed decisions regarding targeted interventions, prioritize restoration areas, and develop effective long-term conservation plans for the hirola antelope.

1.4 Study Area & Study Period

The hirola antelope's population is currently limited to a small geographic range in eastern Kenya which serves as the study area for this project (Ali et al., 2018). Bordered by Somalia to the east and the Tana River to the west, the study area is largely located within Garissa County and encompasses 18,811 km² (Figure 1). It is comprised of well-drained sandy soils with an elevation between 40 – 250 meters above sea level (Ali et al., 2018). This region is semi-arid, with a long rainy season from April to June and a short rainy season from November to December. There is a long dry season from July to October and a short dry season from January to March between the wet seasons (Ali et al., 2018). Historically dominated by rangeland habitat, the hirola's habitat is experiencing significant encroachment of woody vegetation due to several factors, including extirpation of elephants and overgrazing by livestock (Ali et al., 2018). This woody cover has increased by more than 250% since the mid-1980s (Ali et al., 2018). As grazers, hirola depend on rangeland habitats making rangeland restoration a key component for conservation efforts (Ali et al., 2018). Our project focuses on studying the feasibility of using remote sensing techniques to characterize woody vegetation encroachment over time and space to support ongoing restoration efforts. We selected the study period 1986 – 2025 to coincide with the increase in woody cover and study recent spatiotemporal trends in woody vegetation expansion.



Basemap Credit: ESRI ArcGIS Pro, Earthstar Geographics, USGS, and CGIAR

Figure 1. Map depicting geographic extent of the study area and vegetation data provided by project partners.

2. Methodology

We developed woody vegetation time-series maps, and a woody vegetation change map for our study area by integrating multiple Earth observation satellites and datasets. To achieve this, we analyzed three key datasets: (1) Earth observations from NASA's Landsat satellites (1989–2025) to track woody vegetation cover over time through Tasseled Cap Transformation (TCT) and Normalized Difference Vegetation Index (NDVI); (2) NASA's Shuttle Radar Topography Mission (SRTM) data to understand topographic influences on woody encroachment as well as distance to nearby communities and water bodies; and (3) Esri Wayback imagery data to generate random sample points within our study area and classify each based on its woody cover percentage.

2.1 Data Acquisition

The data acquisition process for the woody vegetation time-series mapping involved locating the appropriate satellite imagery to support the detection of woody encroachment in our study area. We obtained Landsat 5, 8, and 9 satellite imagery from USGS Earth Explorer. We downloaded January scenes from Collection-2 Level-2 Landsat 5 Thematic Mapper (TM), Landsat 8 Operational Land Imager (OLI), and Landsat 9 OLI-2 for the years 1989, 2017, and 2023 respectively (Table 1) after filtering for scenes with less than 5% cloud cover due to higher cloud cover in our study area. The Collection-2 Level-2 data uses surface reflectance algorithms to correct for temporally, spatially, and spectrally varying scattering and absorbing effects of atmospheric gases, aerosols, and water vapor. The January dates across all three years were selected based on low-to-no cloud cover during the long January – March dry season for the terrestrial portion of the image.

Table 1
List of Earth observation data utilized for this project.

Sensor	Level	Temporal Resolution	Date(s)	Data	Spatial Resolution	Project Use	Temporal Coverage
Landsat 5 TM	Level 2	16 days	1987/01/26	Bands 1-7	30 m	Derive NDVI and TCT	1987
Landsat 8 OLI	Level 2	16 days	2017/01/12	Bands 2-7	30 m	Derive NDVI and TCT	2017
Landsat 9 OLI-2	Level 2	16 days	2023/01/21	Bands 2-7	30 m	Derive NDVI and TCT	2023
ESRI Wayback Imagery	N/A	N/A	2017/03/29 2025/01/30	WMTS	15 cm	Derive Training Data	2017 & 2025
Shuttle Radar Topography Mission	N/A	N/A	2000	Elevation	30 m	Derive Elevation	2000

We acquired Esri Wayback Imagery for the years 2017 and 2025 as well. This imagery is a digital archive of the World Imagery basemap from 2014 – 2025 with high resolution ranging from 1.9 centimeters (cm) to 150 meters (m). High resolution imagery was necessary to perform ocular estimates of woody cover throughout our study area to use as training data for the Random Forest model. We chose the imagery date 2017-03-29 as our earliest timeframe. This was the earliest imagery date within the long dry season with high enough resolution. This year also matched the Landsat imagery acquired for 2017. Similarly, we used the date 2025-01-30 as it was the most recently available high-resolution imagery within the dry season at the time of the analysis and within a two-year range of the Landsat imagery acquired for 2023. These long dry season dates ensured consistency with the Landsat imagery which were acquired for the month of January which is the start of the long dry season.

The team also incorporated SRTM data from NASA EarthData which provided a near-global coverage of digital elevation with a spatial resolution of 1 arc-second (approximately 30 meters). We used this data to examine elevation variability in our study area and assess potential correlation with the expansion of woody vegetation over time. Lastly, we incorporated field data on woody vegetation locations collected in 2015 by our partner organization. This dataset included 40 unique woody vegetation locations along with their species-specific information. Dominant woody species sampled are included in Table A1. These data points were helpful in supporting further analysis of woody vegetation dynamics and served as a critical reference for understanding the distribution of woody vegetation in our study area. Our partner also provided us with point locations collected in 2020 delineating areas with high *Prosopis juliflora* cover. However, these point locations were located along the Tana River outside of the study area and mainly along trails and roads. Therefore, we did not include these points in our analyses, as they were not representative of the study area and would introduce bias into the model.

2.2 Data Processing

We processed Landsat 5, 8, and 9 Collection-2 Level-2 scenes accessed through USGS Earth Explorer in ArcGIS Pro. The data was converted from 16-bit integer to floating point using a scaling factor and additive offset. We selected bands 2–7 (Blue, Green, Red, Near Infrared [NIR], Short-wave Infrared 1 [SWIR1], and Short-wave Infrared 2 [SWIR2]) to calculate NDVI and TCT which helped to enhance the differences

between woody and non woody vegetation. Maximum NDVI composites were calculated by combining the red and near infrared (NIR) bands (Equation 1; Kriegler et al., 1969) for the years 1987, 2017 and 2023 allowing a detailed investigation of the shrub encroachment over the years.

$$NDVI = \frac{NIR - Red}{NIR + Red} \tag{1}$$

Our data processing also involved calculating TCT of the Landsat bands to derive wetness, greenness and brightness coefficients. To maintain consistency, we chose to extract TCT using the same 3 years as our NDVI calculations: 1987, 2017 and 2023. For 1987, we used bands 1–7 from Landsat 5 TM applying coefficients from Crist & Cicone, 1984 (Table A4), which were multiplied with their respective bands to compute wetness, greenness, and brightness. For 2017 and 2023, we used bands 2–7 from Landsat 8 and 9 OLI following the methodology of Baig et al., 2014 (Table A5), where the coefficients were also multiplied with the respective bands to derive the TCT components.

SRTM from NASA EarthData provided elevation, aspect and slope data which the team used to analyze terrain characteristics of the study area. By integrating the SRTM layer, the team assessed patterns in which topographic variations influence the encroachment of woody vegetation thus inhibiting the spread of herbaceous grassland vegetation. We overlayed the woody vegetation change map with elevation, aspect and slope to evaluate whether topography is driving shifts in woody cover, such as increased vegetation in lowland areas or decrease in steep slopes.

To develop training data for the Random Forest Model, we utilized ArcGIS Pro Version 3.3.0 to generate 300 random points throughout the study area. Then we created 30 x 30 m square plots to remain consistent with the 30 m resolution of the Landsat imagery using the random point as the center of the plot. We split each plot into four quadrants to increase the accuracy and efficiency of our woody cover estimates (Table A2). We used the Esri Wayback Imagery for each year as a basemap and overlaid the sampling plots. The coordinates of the point and associated plot number were recorded in a database. Each team member reviewed 75 plots for each year at a 1:800 m scale and estimated the woody vegetation cover within each plot. Vegetation cover, which we defined as green textured shrub or trees, was estimated to the nearest 5–10% visually and then recorded. Plots with reduced visibility or low resolution were replaced with an X and eliminated from the training data set. For accuracy assessment, plots were cross-referenced by another team member by choosing 10 plots at random and ensuring vegetation estimates remained within a 5–10% range of each other. Inconsistent plot estimates were presented among the whole team to review. Possible factors that influenced the original estimate were discussed (poor resolution, cloud cover, shadows, etc.) and woody cover was re-evaluated as a group until a consensus on the percentage was reached by all members.

2.3 Data Analysis

Given the complex and heterogenous landscape in our study area due to the arid and semi-arid climatic conditions, the team analyzed the datasets using a Random Forest (RF) classifier model. This model is robust at handling high-dimensional data and has the ability to manage non-linearity and the complex interactions of variables. Our RF model proved ideal for mapping woody vegetation cover over the years, as it was effective in monitoring and predicting encroachment of woody vegetation by integrating multi-temporal satellite imagery. NDVI and TCT were integrated into the model as independent (predictor) variables by using their spectral information to predict the spatial distribution of woody vegetation. We used field-estimated woody cover percentages from georeferenced points as a dependent (response) variable since they represented the actual locations with known woody vegetation.

Next, we trained the model using these predictors and the response variable. Each point in the field sampling locations had values for woody vegetation cover percentage and binary woody status (threshold at 50% cover) for both 2017 and 2025. Woody cover percentages greater than 50% received a binary value of 1, and those less than 50% received a binary value of 0. We integrated these field measurements with remote sensing

indices extracted at each location, including Brightness, Greenness, Wetness (from TCT), and NDVI values for both periods. Our RF implementation used 800 decision trees (ntree=800) to ensure model stability while capturing the complex ecological relationships present in savanna ecosystems.

To validate model performance, we calculated Root Mean Square Error (RMSE), Mean Absolute Error (MAE), and coefficient of determination (R²). For spatiotemporal change analysis, we applied the trained models to the entire raster stack covering the study area at 30 m resolution. This produced woody vegetation cover maps for 2017 and 2025, allowing for change detection analysis by calculating the difference between periods.

3. Results

3.1 Analysis of Results

3.1.1 Vegetation Indices

We examined changes in vegetation from 1987 to 2023 by comparing NDVI and TCT indices derived from Landsat 5, 8 and 9 imageries. By comparing these indices, the team was able to have a spatio-temporal detailed view of when and to what extent woody vegetation had encroached or retreated in the landscape. NDVI results computed with clouds exhibited a gradual increase in vegetation, especially in the southern region, from 1987 to 2023 (Figure 2). A further analysis of NDVI threshold by comparing results derived from NDVI midpoint where woody vegetation cover exceeded 50% revealed the following woody vegetation cover; 61% (7,733 km²) in 1987, 54% (6,757 km²) in 2017 and 72% (9,009 km²) in 2023 (Appendix Table A2). Also, NDVI histograms revealed that the majority of the study area has moderate to high vegetation cover, with fewer areas exhibiting very low NDVI values (Appendix Figures B2–B4). With these NDVI maps, our team was able to gain valuable insights into shifts in vegetation health and dynamics to enable further analysis.

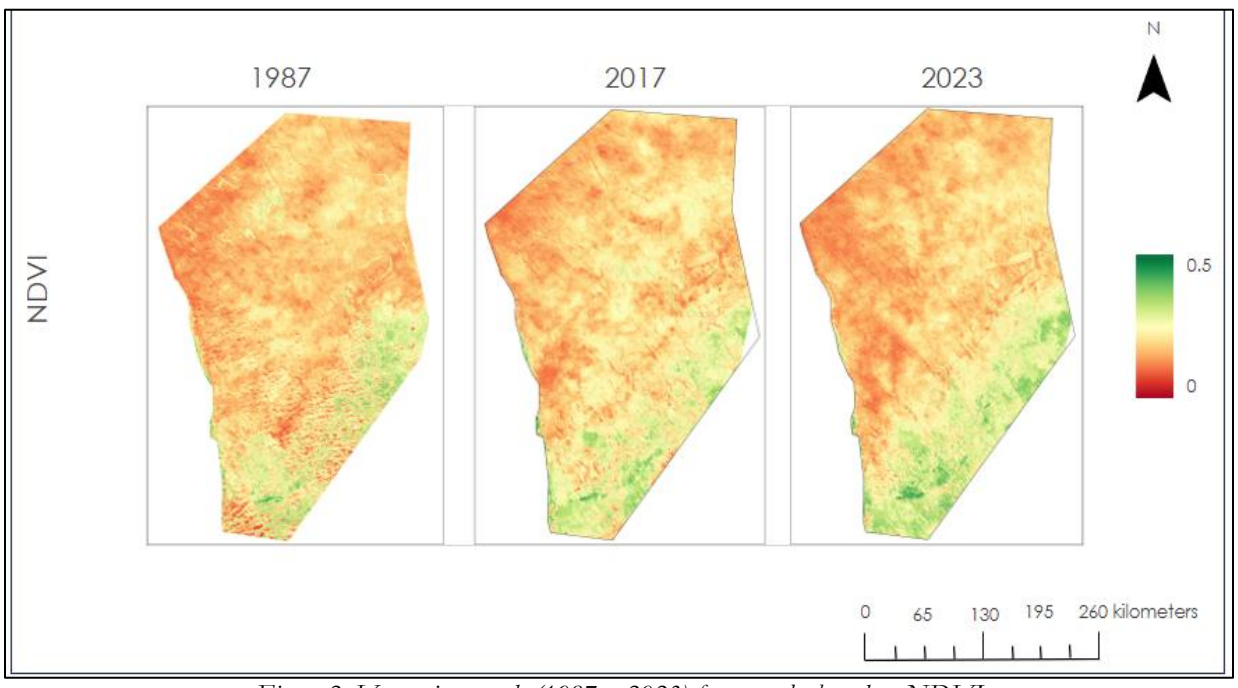


Figure 2. Vegetation trends (1987 – 2023) from results based on NDVI

Similarly, TCT indices computed with clouds, particularly the brightness, greenness, and wetness components, revealed additional details about landscape changes. The TCT greenness index showed an increasing trend, consistent with NDVI results, further confirming vegetation expansion in the southern region of the study area (Figure 3). TCT brightness indicated low values in the southern regions which is representative of dense vegetation, this in agreement with the greenness results. On the other hand, TCT

wetness highlighted a decline in moisture availability in the southern region and an increase in the north over time. The integration of NDVI and TCT indices allowed for a more comprehensive assessment of vegetation changes, offering a nuanced view of land cover transformation in the study area.

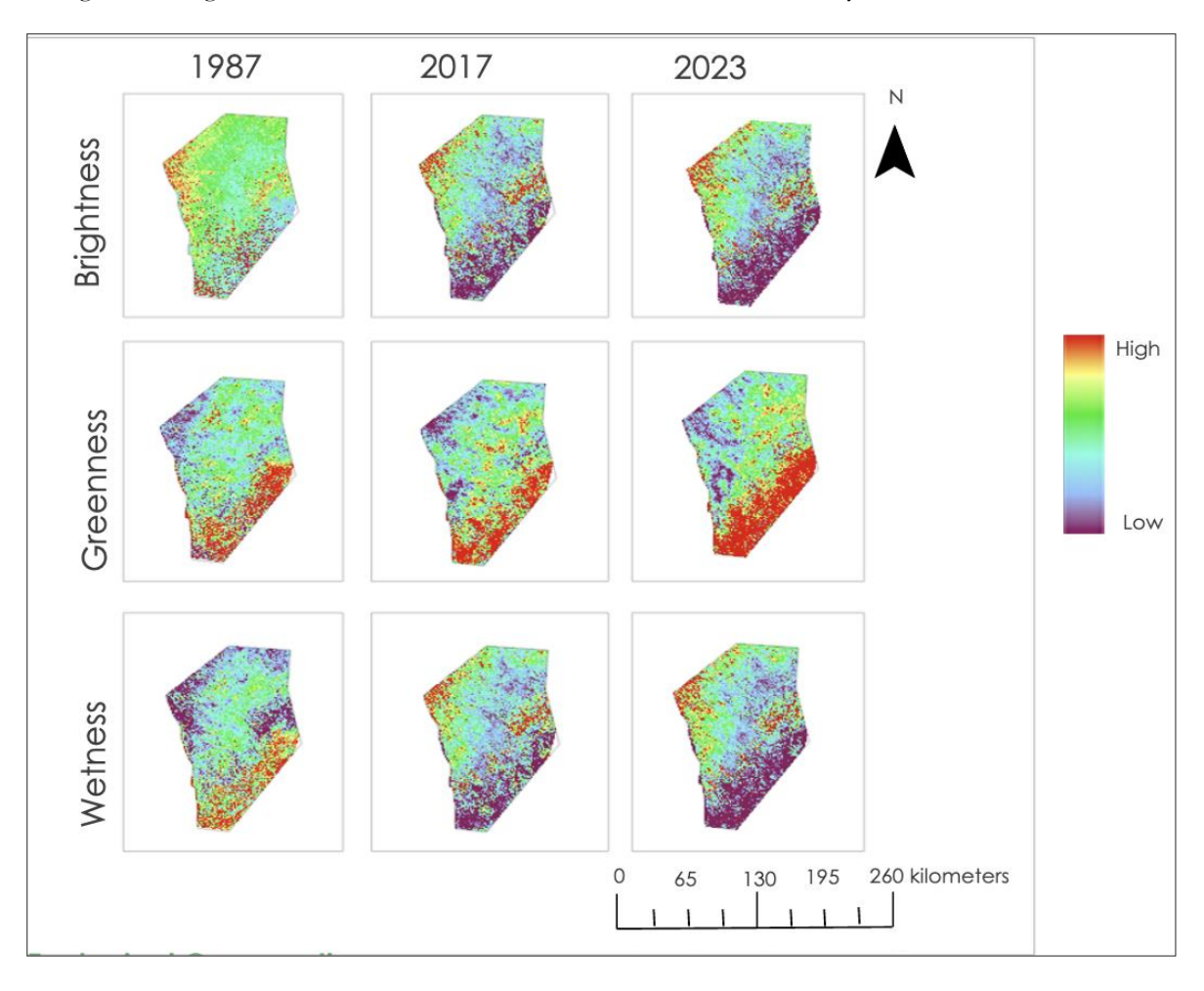


Figure 3. TCT trends (1987–2023) from results based on the brightness, greenness and wetness indices

3.1.2 Woody Vegetation Cover

Our analysis of woody vegetation cover integrated spectral data from satellite sensors with ground-truth observations to create a comprehensive characterization of landscape changes. The Random Forest algorithm we employed is particularly well-suited for this application as it creates multiple decision trees from samples of the training data, with each tree casting a "vote" for the predicted class. The model achieved an adjusted R² value of 0.913 and an RMSE of 6.5%, indicating high prediction accuracy. This ensemble approach reduces overfitting and handles the complex, non-linear relationships between spectral indices and woody cover.

The maps in Figure 4 show the continuous woody cover percentages across our study area for three key periods. The orange-brown color scale represents woody cover percentage, with darker areas indicating higher woody vegetation density. In the 1987 maps, woody cover density ranged from 40% to 90%, with a more uniform distribution and generally lower density in northern portions. By 2017, the pattern shifted to a range of 20% to 80%, with increased woody cover particularly in central and northern regions as darker orange tones became more prevalent. The 2025 map shows further intensification compared to 2017, with the darkest orange areas expanding throughout the study area.

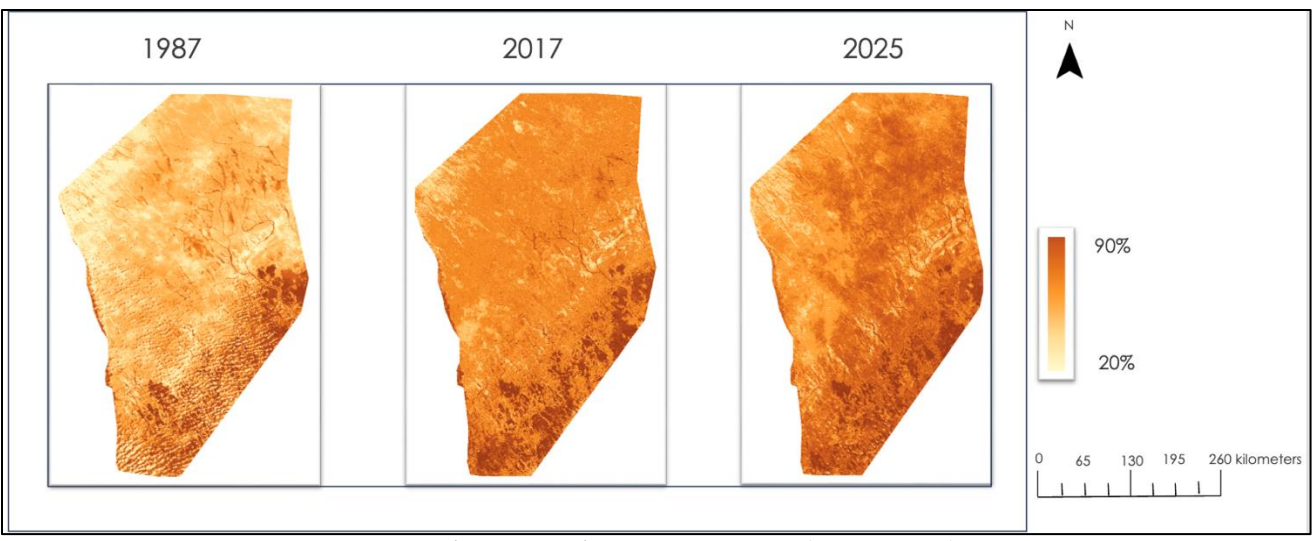


Figure 4. Woody vegetation density time series map (1987 – 2025)

The spatial distribution revealed consistent patterns across periods, with the highest woody vegetation concentrations along drainage networks and in southeastern portions. While the northern regions remained lighter in the earlier periods, the recent maps also reflect the expansion of woody vegetation towards previously untouched open grasslands.

3.1.3 Woody Vegetation Change

To quantify vegetation change accurately, we developed binary classification maps that highlighted areas of significant transformation across different periods. This technique involved applying thresholds to our continuous woody cover predictions and calculating the differences between time points. We used both pixel-by-pixel comparisons and aggregate statistics to characterize the nature and extent of woody vegetation dynamics throughout the study region (Figure 5).

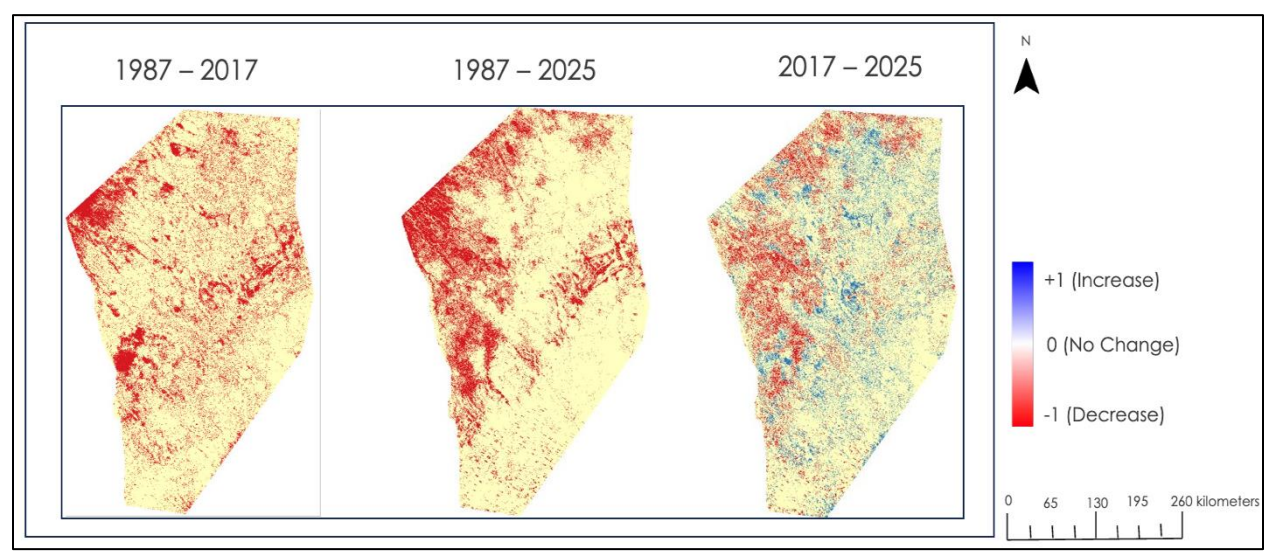


Figure 5. Patterns of binary change in woody vegetation within the study area (1987 – 2025)

Figure 5 illustrates the binary change maps, revealing significant shifts in woody vegetation cover across different periods. The 1987–2017 and 1987–2025 maps show predominantly red areas, indicating apparent woody cover decrease. However, these earlier comparisons should be interpreted cautiously due to limitations in ground truth data and high-resolution imagery from the 1987 period. The 2017–2025 map provided the

most reliable analysis, displaying a complex pattern with both blue areas (woody vegetation increase) and red areas (decrease), revealing the dynamic nature of recent vegetation change.

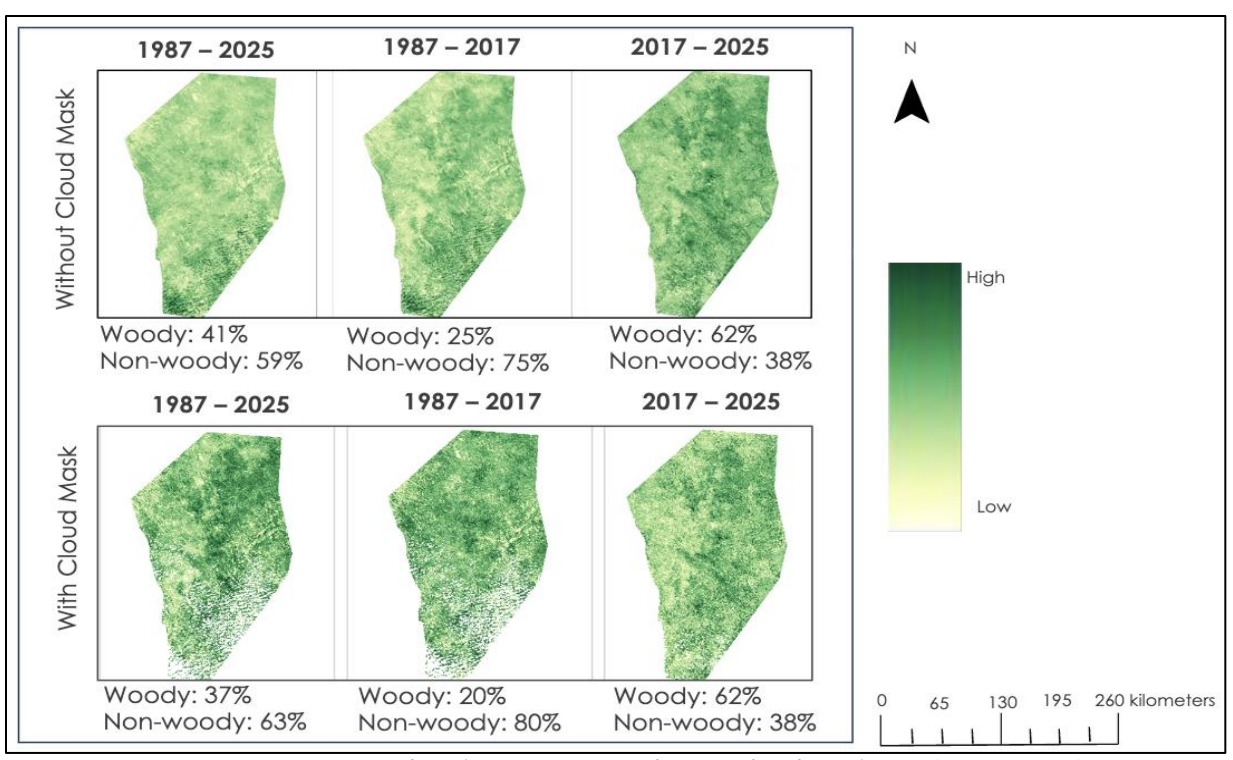


Figure 6. Progression of woody vegetation encroachment within the study area (1987 – 2025)

The encroachment progression maps in Figure 6 directly quantify woody vegetation differences between periods, with darker green indicating greater prevalence. The maps are presented both with and without cloud masking to ensure analytical transparency. With cloud masking applied, the 1987–2025 map shows woody cover at 37% (approximately 1.48 million acres), while the 2017–2025 map reveals a strikingly rapid encroachment over just eight years, with woody vegetation increasing to 62% (2.9 million acres). Notable hotspots of woody encroachment appear in southern and central regions, coinciding with critical hirola habitat zones. This spatial pattern suggests encroachment is spreading from existing woody patches outward into previously open grasslands, directly threatening the grassland habitat preferred by the critically endangered hirola antelope.

3.2 Errors & Uncertainties

We were unable to obtain high resolution imagery of the area within the 1980s or 1990s to create the training data for these date ranges. Therefore, we applied the 2017 model to the TCT values derived from the 1987 Landsat imagery. This approach allowed us to analyze woody vegetation trends across a four-decade timespan, but it did affect the reliability of the prediction of woody vegetation change from 1987–2017 and 1987–2025. Our prediction also did not consider how large-scale climatic effects have affected woody encroachment over this time period. For example, in the early 2000s, seasonal rains failed for two consecutive years in Kenya, leading to a severe drought crisis (UNICEF, 2000). This and the lack of ground truth data could explain the low increase in woody vegetation from 1987–2017. The imagery available for the earlier part of the study period also contained high amounts of cloud cover, even in the dry season. This higher cloud cover in the 1987 imagery was incorporated in the cloud mask that was applied in the analysis of woody encroachment over time. This could have affected the predictions for the later part of the study area, 2017–2025.

Additionally, we were not able to use the partner's *Prosopis juliflora* data to create a prediction model solely for this species because of lack of usable imagery during the wet season and representative *Prosopis juliflora* points. The imagery available was unusable due to the high amount of cloud cover that obscured large portions of the study area. *Prosopis juliflora* is a woody evergreen species that flowers repeatedly (Kamiri et al., 2024). These characteristics make it distinguishable from other species, but imagery from wet and dry seasons would be needed to validate predictions in our model. Further, we were unable to incorporate the ground truth data collected by the partner to a prediction model because of the habitat, location, and extent of the data. The points were collected in areas where *Prosopis juliflora* is the densest along the Tana River. This floodplain habitat is different than the semi-arid habitat of our study area. They also fall outside of our study area and are mainly along roads and trails. These factors would have introduced bias into our model, creating an inaccurate prediction of its distribution within the study area.

4. Conclusions

4.1 Interpretation of Results

By combining NASA Earth observations (Landsat 5, Landsat 8, Landsat 9, and SRTM) and woody cover point data derived from supplemental high resolution satellite imagery (Esri Wayback Imagery), it was feasible to map out the historical patterning of woody encroachment across semi-arid savannahs of Kenya. In Garissa County, our NDVI and TCT findings suggest an increase in woody encroachment over the past four decades, with dominance over the southeast and historical spreads into the northwest. It should be emphasized that due to the limited data availability, these results should be considered preliminary and interpreted with caution. Continuing, the trends present in this study may be utilized to reinforce prevention and mitigation efforts by allowing our partner to anticipate future trends in woody encroachment based on these historic characteristics. For example, the NDVI time-series maps could help visualize the general vegetation trend and identify different locations that may be undergoing a transition. Additionally, the significance of these results may help inform restoration and removal operations by highlighting areas of high concentration throughout the region (e.g. southeast, proximity to streams) to enhance the efficiency of on-the-ground prioritization. For example, the brightness, wetness, and greenness tasseled cap transformation maps could help track vegetation shifts over time, which can help detect areas in need of grassland restoration. Thus, the woody vegetation maps could be used to help pinpoint specific regions that are experiencing a higher influx of woody vegetation encroachment that may overtake grassland habitats vital to the survival of the hirola antelope.

4.2 Feasibility & Partner Implementation

The feasibility of using NASA Earth observations to analyze woody shrub encroachment in semi-arid regions like Garissa County proves to be optimistic, despite the limitations and uncertainties associated. However, it was not feasible to identify species-specific vegetation, like *Prosopis juliflora*, or to map out these regions during wet seasons. To further our methodology, choosing earlier time periods and gathering more ground truth data may allow for clearer, more accurate results. Our resulting metrics support our partner's knowledge. In conjunction with our representative maps infused with vegetation indices (e.g., NDVI) and other topographic layers, the partner may be able to better showcase and communicate the issue of woody encroachment to the local communities most affected by grassland degradation and the decline of the hirola.

5. Acknowledgements

We would like to extend our sincere gratitude to our partners at the Hirola Conservation Program, Dr. Abdullahi Ali, Sangale Edwin, and Mohamed Hussein, for sharing their time, field data, and expertise of the region with us. We also want to thank our science advisors from the Natural Resource Ecology Laboratory at Colorado State University, Nicholas Young and Anthony Vorster, who provided crucial research support throughout the term. We are also grateful to our center lead, Katie Miller, for her help and encouragement during our DEVELOP experience and to our Project Coordination Fellow, Isabel Tate, for her beneficial feedback. Lastly, a special thanks to members of the Langley Research Center, Dr. Kent Ross and Dr. Xia Cai, whose incredible expertise provided us with valuable knowledge that strengthened our project.

Any opinions, findings, and conclusions or recommendations expressed in this material are those of the author(s) and do not necessarily reflect the views of the National Aeronautics and Space Administration. This material is based upon work supported by NASA through contract 80LARC23FA024.

6. Glossary

Desertification – Process in which vegetation in semi-arid lands decreases and disappears, typically as a result of climatic variations such as drought, or human activities such as intensive agriculture practices.

Earth observations – Satellites and sensors that collect information about the Earth's physical, chemical, and biological systems over space and time.

Invasive species – A species that is introduced to an area where it is not considered native and harms its new environment by outcompeting and overwhelming native species.

Landsat 5 TM – A satellite sensor (Thematic Mapper) operational from 1984–2013, capturing multispectral imagery for earth observation.

Landsat 8 OLI – A satellite sensor (Operational Land Imager) operational since 2013, delivering advanced, high-quality multispectral and thermal imagery.

Landsat 9 OLI-2 – A satellite sensor operational from 2021, an upgraded version of the Operational Land Imager for enhanced earth observation.

NDVI – Normalized Difference Vegetation Index; a remote sensing index that uses red and near-infrared bands to assess vegetation health and greenness.

R² (Coefficient of determination) – A statistical measure that indicates the proportion of variance in the dependent variable explained by the independent variables in a regression model.

Random Forest (RF) – A machine learning algorithm that generates multiple decision trees from random subsets of the data and aggregates their predictions.

Rangeland habitat – Ecosystems dominated by grasses, shrubs, or open woodlands, primarily used for livestock grazing and wildlife habitat.

Remote sensing – Process of detecting and monitoring the physical characteristics of an area from a satellite or aircraft to measure its reflected and emitted radiation from a distance.

Rinderpest – A highly contagious and fatal viral disease that affected cattle and other domestic and wild ruminants, that was declared eradicated worldwide in 2011.

Semi-arid – Landform or habitat characterized by scrubby vegetation and experiences little yearly rainfall. **TCT** – Tasseled Cap Transformation, a remote sensing index that converts multispectral imagery bands to new bands corresponding to brightness, greenness, and wetness used to assess soil and vegetation.

Woody encroachment – Process in which woody species invade ecosystems that were historically free of woody shrubs or trees like grasslands for example, leading to the conversion or fragmentation of habitat.

7. References

Ali, A., Amin, R., Evans, J., Fischer, M., Ford, A., Kibara, A. & Goheen, J. (2018). Evaluating support for rangeland-restoration practices by rural Somalis: An unlikely win-win for local livelihoods and hirola antelope?. *Animal Conservation*, 22, 1-11 https://doi.org/10.1111/acv.12446

- Ali, A., Ford, A., Evans, J., Mallon, D., Hayes, M., King, J., Amin, R., & Goheen, J. (2017). Resource selection and landscape change reveal mechanisms suppressing population recovery for the world's most endangered antelope. *Journal of Applied Ecology*, *54*(6), 1720–1729. https://doi.org/10.1111/1365-2664.12856
- Baig, M. H. A., Zhang, L., Shuai, T., & Tong, Q. (2014). Derivation of a tasselled cap transformation based on Landsat 8 at-satellite reflectance. *Remote Sensing Letters*, *5*(5), 423–431. https://doi.org/10.1080/2150704X.2014.915434
- Breiman, L. (2001). Random Forests. *Machine Learning*, 45(1), 5–32. https://doi.org/10.1023/a:1010933404324
- Crist, E.P. and Cicone, R.C. (1984) 'A Physically-Based Transformation of Thematic Mapper Data---The TM Tasseled Cap. *IEEE Transactions on Geoscience and Remote Sensing*, GE-22(3), pp. 256–263. https://doi.org/10.1109/tgrs.1984.350619.
- Esri (2018). World Imagery (Wayback 2017-03-29) [Data set]. Esri Wayback Imagery. Retrieved February 27, 2025, from https://arcg.is/1yWvuD
- Esri (2025). World Imagery (Wayback 2025-01-30) [Data set]. Esri Wayback Imagery. Retrieved February 27, 2025, from https://arcg.is/liLy4f
- Higginbottom, T. P., Symeonakis, E., Meyer, H., & Sebastian. (2018). Mapping fractional woody cover in semi-arid savannahs using multi-seasonal composites from Landsat data. *Isprs Journal of Photogrammetry and Remote Sensing*, 139, 88–102. https://doi.org/10.1016/j.isprsiprs.2018.02.010
- Hirola Conservation Program (HCP). (2024). 2023-2024 Annual Report. Hirola Conservation Program, 3. https://hirolaconservation.org/wp-content/uploads/2024/12/HCP_ANNUAL_REPORT_2023_Final.pdf
- Jowers, M. J., Queirós, J., Resende Pinto, R., Ali, A. H., Mutinda, M., Angelone, S., Alves, P. C., & Godinho, R. (2020). Genetic diversity in natural range remnants of the critically endangered Hirola Antelope. *Zoological Journal of the Linnean Society*, 190(1), 384–395. https://doi.org/10.1093/zoolinnean/zlz174
- Kamiri, H. W., Choge, S. K., & Becker, M. (2024). Management Strategies of *Prosopis juliflora* in Eastern Africa: *What Works Where?*. *Diversity*, 16(4), 251. https://doi.org/10.3390/d16040251
- Kosgei, S., Mbaabu, P. R., & Muturi, G. M. (2022). Management and control of the invasive prosopis juliflora tree species in Africa with a focus on Kenya. *Prosopis as a Heat Tolerant Nitrogen Fixing Desert Food Legume*, 67–81. https://doi.org/10.1016/b978-0-12-823320-7.00024-9
- Kriegler, F., Malila, W., Nalepka, R., & Richardson, W. (1969). Preprocessing transformations and their effect on multispectral recognition. Proceedings of the 6th International Symposium on Remote Sensing of Environment. Ann Arbor, MI: University of Michigan, 97-131.

- Ng, W.-T., Meroni, M., Immitzer, M., Böck, S., Leonardi, U., Rembold, F., Gadain, H., & Atzberger, C. (2016). Mapping Prosopis spp. with Landsat 8 data in arid environments: Evaluating effectiveness of different methods and temporal imagery selection for Hargeisa, Somaliland. *International Journal of Applied Earth Observation and Geoinformation*, 53, 76–89. https://doi.org/10.1016/j.jag.2016.07.019
- Sheng, L., Huang, Jf. & Tang, Xl. A tasseled cap transformation for CBERS-02B CCD data. *J. Zhejiang Univ. Sci.* B 12, 780–786 (2011). https://doi.org/10.1631/jzus.B1100088
- UNICEF. (2000). UNICEF Kenya Drought response update 6 Jul 2000 kenya. ReliefWeb. https://reliefweb.int/report/kenya/unicef-kenya-drought-response-update-6-jul-2000
- Young, N. E., Anderson, R. S., Chignell, S. M., Vorster, A. G., Lawrence, R., & Evangelista, P. H. (2017). A survival guide to Landsat preprocessing. *Ecology*, 98(4), 920–932. https://doi.org/10.1002/ecy.1730

8. Appendices

Appendix A

Table A1

Dominant woody vegetation species sampled in partner data.

Species	Local Name
Acacia reficiens	Riig
Dobera glabra	Garas
Acacia bussei	Sarman
Combretum hereroense subsp. volkensii	Qoqon
Grewia tenax	Deka
Cordia sinensis	Marer
Salvadora persica	Adhei
Commiphora africana	Damaja
Acacia mellifera	Bil-in
Acacia hamulosa	Bil-il

Table A2
Forest Cover Estimates by Model and Year

Woody Vegetation Cover (km²) Area projected with 50% cover					
Variable	Year (NDVI Threshold)				
Variable	1987 (>0.19)	2017 (>0.20)	2023 (>0.21)	2025	
NDVI Threshold	7,733 km ² (61.8%)	6,757 km ² (54%)	9,009 km ² (72%)	X	
Year Specific Model	X	8,793 km ² (48%)	X	10,695 km ² (56%)	
Single Model	15,900 km ² (84.9%)	15,033 km ² (80.3%)	15,113 km ² (80.5%)	17,354 km ² (92.7%)	

Table A3
Forest Cover Change Estimates by Model and Year

Woody Cover Change (km²)				
	1987–2025	1987–2017	2017–2023	
TCT Threshold (>0)	6,561 km ² (35.3%)	3,355 km ² (18%)	10,970 km ² (59%)	
Year Specific Model	X	X	11,463 km ² (62.3%)	
Single Model	+1,454 km ² (9.1%)	-867 km ² (-5.5%)	+2,321 km ² (12.4%)	

Table A4

Tasseled Cap Transformation parameters for Landsat 5 TM

	Brightness	Greenness	Wetness
Band 1	0.3037	-0.2848	0.1509
Band 2	0.2793	-0.2435	0.1973
Band 3	0.4743	-0.5436	0.3279
Band 4	0.5585	0.7243	0.3406
Band 5	0.5082	0.0840	-0.7112
Band 7	0.1863	-0.1800	-0.4572

Table A5

Tasseled Cap Transformation parameters for Landsat 8 OLI and Landsat 9 OLI-2

	Brightness	Greenness	Wetness
Band 2	0.3029	-0.2941	0.1511
Band 3	0.2786	-0.2430	0.1973
Band 4	0.4733	-0.5424	0.3283
Band 5	0.5599	0.7276	0.3407
Band 6	0.5080	0.0713	-0.7117
Band 7	0.1872	-0.1608	-0.4559

Appendix B



Figure B1. Example of the 30×30 m sample plots created in ArcGIS Pro for our ocular estimates of woody vegetation. This plot overlays 2025-01-30 Esri Wayback Imagery.

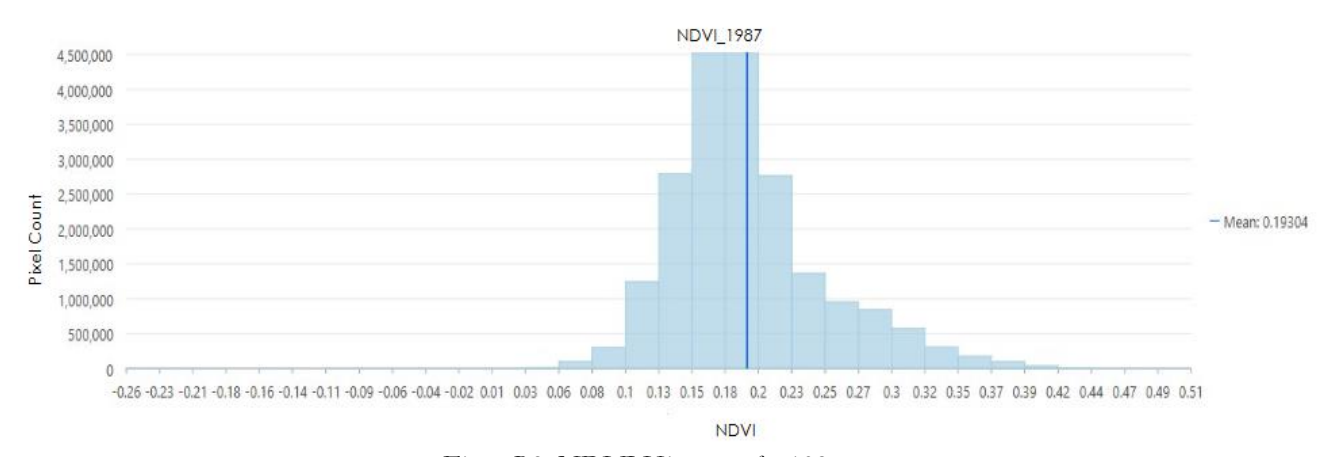


Figure B2. NDVI Histogram for 1987

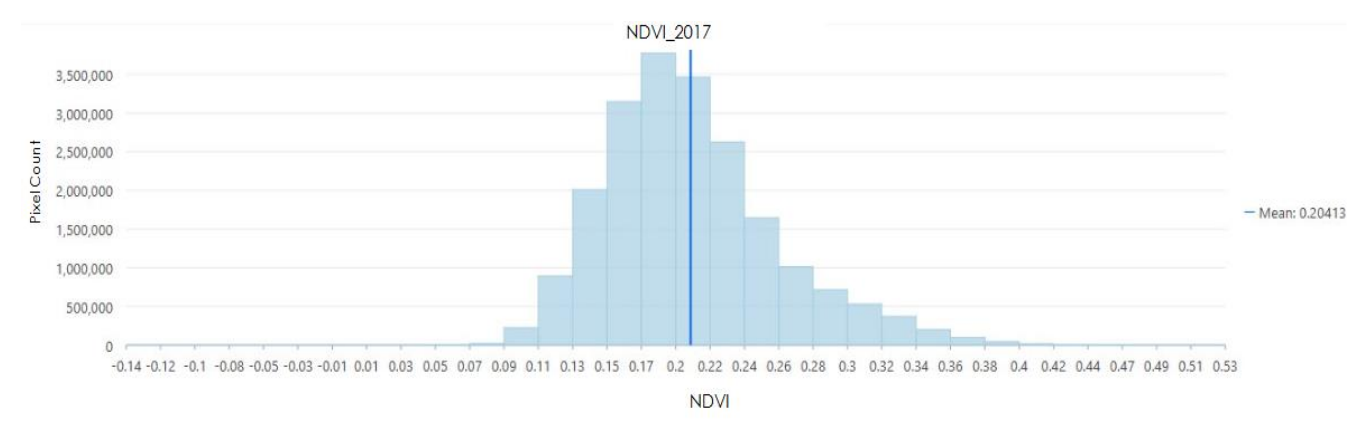


Figure B3. NDVI Histogram for 2017

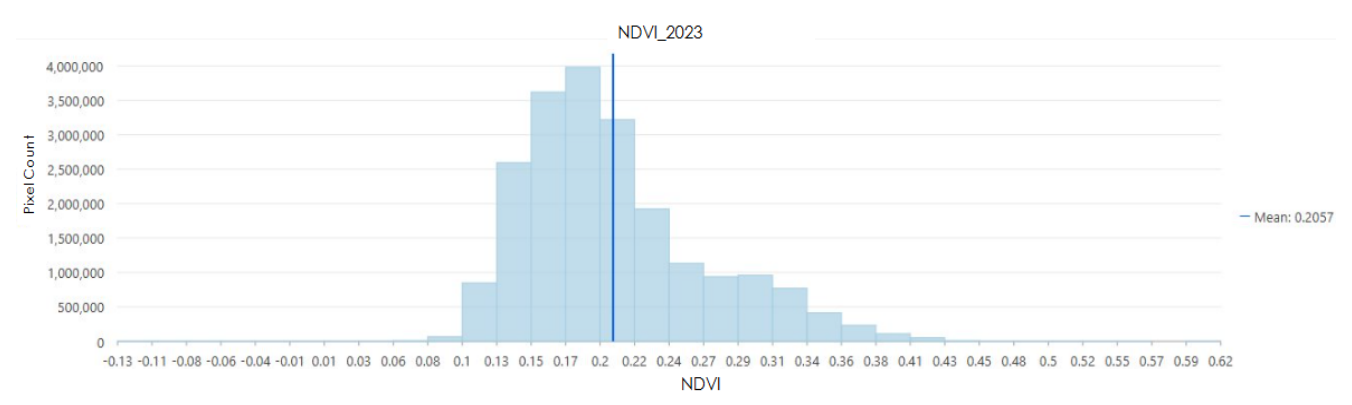


Figure B4. NDVI Histogram for 2023